www.sciencemag.org/cgi/content/full/science.aab2749/DC1

Supplementary Materials for

Retroviruses use CD169-mediated trans-infection of permissive lymphocytes to establish infection

Xaver Sewald,* Mark S. Ladinsky, Pradeep D. Uchil, Jagadish Beloor, Ruoxi Pi, Christin Herrmann, Nasim Motamedi, Thomas T. Murooka, Michael A. Brehm, Dale L. Greiner, Leonard D. Shultz, Thorsten R. Mempel, Pamela J. Bjorkman, Priti Kumar,* Walther Mothes*

*Corresponding author. E-mail: xaver.sewald@yale.edu (X.S.); priti.kumar@yale.edu (P.K.); walther.mothes@yale.edu (W.M.)

Published 2 October 2015 on *Science* Express
DOI: 10.1126/science.aab2749

This PDF file includes:

Other Supporting Online Material for this manuscript includes the following:
(available at www.sciencemag.org/cgi/content/full/science.aab2749/DC1)

Materials and Methods:

Mice

C57BL/6 mice, NOD.Cg-*Prkdc*^{scid} *Il2rg*^{tm1Wjl}/SzJ (NSG) mice and mice expressing cytoplasmic DsRed [Tg(CAG-DsRed*MST)1Nagy/J] (designated RFP^{+} mice) in all nucleated cells were obtained from Jackson Laboratory. *Siglec1*$^{-/-}$ mice (*14*) were from Paul Crocker, University of Dundee. All experiments were approved by the Institutional Animal Care and Use Committees (IACUC) of Yale University, the Massachusetts General Hospital, the Jackson Laboratory and the University of Massachusetts and Institutional Biosafety Committees of Yale University, Massachusetts General Hospital and University of Massachusetts.

Generation of humanized mice

Humanized mice generated by either the HSC or the BLT routes as described previously (*31*) were used in this study. For generating Hu-HSC mice, one- to two-day-old neonatal NSG mice (Jackson Laboratories, Bar Harbor, Maine) were irradiated (100 cGy) and injected through the intracardiac route with 10^5 CD34^{+} hematopoietic stem cells immunomagnetically purified from human umbilical cord blood (National Disease Research Interchange). The generation of humanized BLT (fetal liver/thymus/hematopoietic stem cell-engrafted) mice was performed using human fetal thymus and fetal liver (gestational age between 16 and 20 weeks) tissue from Advanced Bioscience Resources (Alameda, CA). 5-8 week old NSG mice were irradiated with 200 cGy and 1 mm^3 fragments of human thymus and fetal liver were co-transplanted together in the renal subcapsular space. The remaining fetal liver was dissociated into a single cell suspension, and immunomagnetically purified human CD34^{+} cells were injected intravenously via the tail vein into the tissue-transplanted mice. The transplanted mice were tested for engraftment ~10 weeks later by flow cytometric analysis of peripheral blood for human immune cells.

Virus preparation

Full-length Friend MLV viral constructs are based on the pLRB303 plasmid (*32, 33*). MLV Gag-GFP labeled virions were previously described (*19*). MLV constructs lacking Env were generated in the context of the pLRB303 plasmid encoding Gag-GFP by introducing two premature stop codons in Env. MLV Gag-GFP particles containing or lacking Env were generated by transfecting cells with this plasmid in the additional presence of a plasmid expressing MLV GagPol at a ratio of 2:1, respectively (*19*). For reporter virus production HEK293 cells were co-transfected with pLRB303 derived plasmid encoding full-length MLV (WT or ΔEnv) and the additional plasmid pMMP-LTR-GFP expressing cytoplasmic GFP at a ratio of 10:1, respectively. For single round infection experiments pcDNA3 plasmid encoding ecotropic or amphotropic MLV Env were added to pLRB303 MLV ΔEnv and pMMP-LTR-GFP. Viral titers of ecotropic MLV were determined by titrating concentrated virus on the murine T lymphoid cell line S49.1. Viral titers of MLV with amphotropic Env were determined using Jurkat T cells. GFP expression was determined after 24 h by flow cytometry. Ganglioside-depleted virus was generated by treating producer cells with 10 μM PDMP (Sigma) as previously described (*34*). Successful ganglioside depletion of produced virus was confirmed by dot-blot analysis using cholera toxin subunit B-horseradish peroxidase (CtxB-HRP) (Invitrogen). HIV Gag-GFP viruses were generated by transfecting a derivative of the pNL4-3 molecular clone lacking reverse transcriptase and GFP fused to Gag (pCMVNL Gag-GFP ΔRT) in HEK293 cells. We used immortalized (3T3 method) mouse embryonic fibroblasts (MEFs) to produce mouse cell-derived MLV. We generated MEFs stably producing replication competent MLV carrying Gag-GFP by transfecting them with full-length Friend MLV and MLV Gag-GFP expressing constructs using Lipofectamine 2000 (Invitrogen, CA). Cells were grown in roller bottle cultures and

culture supernatant containing virus was harvested every 2 days for a period of 3 weeks. Pooled culture supernatants were sedimented through a 15 % sucrose-PBS cushion at 25,000 x g to obtain concentrated MLV Gag-GFP. For *in vivo* capture experiments the above described viruses were normalized to MLV Gag-GFP WT preparations by western blot analyses using antibodies to GFP.

Flow cytometry

PFA-fixed cells from lymph nodes and spleens were blocked for 15 min in PBS/2 % BSA containing 5 % rat serum and Fc blocking antibody against CD16/CD32 (BioLegend) before staining with antibodies for flow cytometry analysis. Antibodies used in the study: CD19-PE (clone 1D3, BioLegend), CD19-APC (clone 1D3, BioLegend) CD5-AF647 (clone 53-7.3, BioLegend), CD9-AF647 (clone MZ3, BioLegend), CD43-APC (clone S7, BD), IgD-APC (clone 11-26c.2a, BioLegend) CD1d-AF647 (clone 1B1, BioLegend), CD38-APC (clone 90, BioLegend), CD138-APC (clone 281-2, BioLegend), CD3e-APC (clone 145-2C11, BioLegend), CD8-PE (clone 53-6.7, BioLegend), CD4-APC (clone RM4-5, BioLegend), CD11c-APC (clone HL3 or N418, BD or BioLegend), CD11b-APC (clone M1/70, BioLegend), CD169-PE (clone 3D6.112, BioLegend), CD209b/SIGN-R1-APC (clone 22D1, eBioscience), APC-conjugated anti-human CD45 (BD Pharmingen), FITC-conjugated anti-human CD3 (BD Pharmingen), PE-conjugated anti-human CD8 (BD Pharmingen), PerCP/Cy5.5-conjugated anti-human CD4 (BioLegend). Data were acquired on a FACS Calibur, Accuri C6 or LSRII flow cytometer (BD Biosciences) and were analyzed with FlowJo software (Treestar). For retrovirus capture and infection experiments, viable leukocytes were gated for GFP-positive cells based on PBS control samples. Gates were set to 0.01-0.001 % GFP^+ cells of total leukocytes (Fig. 1C). 150,000-900,000 viable cells were acquired for each sample. The number of independent replicates for each experiment is mentioned in the figure legends. Each dot represents a single popliteal lymph node (pLN) or spleen sample.

Retrovirus capture and infection in mice

To quantify virus capture at the draining pLN of C57BL/6 and *Siglec1*$^{-/-}$ mice, fluorescent MLV Gag-GFP, produced in HEK293 cells or MEFs, and HIV Gag-GFP virus particles were concentrated by sedimenting through a 15 % sucrose-PBS cushion. Concentrated virus suspension (25 µl, corresponding to 100,000-400,000 infectious units) was subcutaneously (s.c.) injected into the footpads of mice. Draining pLNs were isolated at indicated time points and prepared for flow cytometry by incubation with Liberase TL (0.2 mg/ml, Roche) and DNase I (20 µg/ml, Roche) for 20-30 min at 37°C followed by passing the tissue through a 70 µm cell strainer. For protease inactivation 10 % FCS was added. Samples were fixed with 4 % PFA and analyzed by flow cytometry. For retrovirus capture at the spleen of C57BL/6 and *Siglec1*$^{-/-}$ mice, concentrated virus (200 µl) was injected into the tail vein and the spleen was isolated 30 min after virus injection. For splenocyte preparation, spleens were digested with Liberase TL (0.2 mg/ml, Roche) for 15 min at 37°C, passed through a 70 µm cell strainer, treated with red blood cell lysis buffer, and fixed with 4 % PFA before flow cytometry analysis. For blocking experiments, 1 or 10 µg of antibodies to CD169 (clone 3D6.112) or rat IgG2a isotype control were injected s.c or into the tail vein 30 min prior to virus injection to block CD169 at the pLN or spleen, respectively. For *in vivo* infection experiments 4 x 10^4 infectious units (I.U.) of MLV LTR-GFP variants were s.c. injected into the footpad of C57BL/6 or *Siglec1*$^{-/-}$ mice and the draining pLNs were analyzed 2 days post infection by flow cytometry. MLV infection of splenocytes was analyzed after i.v. injection of 1 x 10^5 I.U. of MLV LTR-GFP. The spleen was isolated 2 days post infection and processed for analysis as described above. For single round infection experiments, MLV LTR-GFP reporter virus was produced with MLV ΔEnv genome in the additional presence of pcDNA3 plasmid encoding ecotropic Env. MLV-infected leukocytes (GFP-expressing cells) were characterized by flow cytometry.

HIV capture and infection in humanized mice

As the development of lymph nodes in humanized mice (NSG) is rare, we performed all experiments with spleen as the target lymphoid organ. To study the effect of CD169 on HIV capture and infection in the spleen of humanized mice, 25 µg each of *in vivo*-use approved antibodies blocking human CD169 (clone 7-239) and mouse CD169 (clone 3D6.112) or their corresponding isotype antibodies (clones MOPC-21 and RTK2758) (BioLegend) were injected intravenously. To analyze CD169-dependent capture at the spleen of BLT mice, antibodies were injected 30 minutes prior to HIV Gag-GFP. PFA-fixed splenocytes were analyzed for HIV Gag-GFP capture 30 minutes later by flow cytometry. To study HIV infection in Hu-HSC mice, blocking CD169 and control antibodies were injected on day -1, 30 minutes prior to HIV-1 BaL injection (100,000 I.U.) (day 0) and on day 2. Mice were euthanized on day 3 and spleens were harvested aseptically. Single cell suspension of splenocytes were prepared by digesting the spleen with Liberase TL (0.2 mg/ml, Roche) for 15 min at 37°C followed by passage through a 70 µm cell strainer and treatment with red blood cell lysis buffer. $CD8^+$ T cells were depleted from splenocytes by positive selection using EasySep immunomagnetic cell selection kit (StemCell Technologies). $CD8^+$ T cell-depleted splenocytes were cultured in 96-well plate with RPMI/10% fetal bovine serum, 100 µg/mL streptomycin and 100 UI/mL penicillin (Sigma), phytohaemagglutinin (1 µg/mL; Sigma) and recombinant interleukin-2 (20 U/mL; Chiron) to promote T cell activation and HIV replication. Supernatants were harvested after ten days of *ex vivo* culture and the released HIV-1 infectivity was measured using TZM-bl indicator cells via firefly luciferase assay.

Intravital microscopy and image analysis

Retrovirus capture and transfer was monitored at the popliteal lymph node of anesthetized mice essentially as previously described (*19*). Where indicated, B-1 cells or naïve B cells were adoptively transferred s.c. or i.v. 18 - 24 h before imaging experiments. Mice were initially anesthetized by intraperitoneal injection of a ketamine and xylazine mixture and subsequently with nebulized isoflurane/O_2 gas mixture. Animals were immobilized on a custom-built stage and the right popliteal lymph node was surgically prepared. The lymph node was immersed in saline and covered with a glass coverslip. Temperature of the lymph node was maintained at 37°C during imaging. To visualize retrovirus capture *in vivo*, MLV Gag-GFP and HIV Gag-GFP particles (100,000-400,000 I.U.) were s.c. injected into the footpad of C57BL/6 mice after lymph node surgery and arrival of fluorescent particles was recorded immediately. To quantify infectious synapses and visualize virus transfer, B-1 cells were analyzed 1 h before and up to 4 h after s.c. injection of MLV Gag-GFP (+Env, -Env). For *in vivo* staining of SCS macrophages or $CD11c^+$ DCs, 1 µg of AlexaFluor568 (A568)- or CF568-conjugated antibodies to CD169 (clone 3D6.112) or CD11c (clone N418), respectively, were s.c. injected 30 min after virus injection. To block MLV capture, 1 µg of A568-conjugated antibodies to CD169 was s.c. injected 30 min before virus injection. For higher resolution analysis of retrovirus capture *in vivo*, pLNs were fixed with PLP solution (see Immunohistochemistry paragraph) before microscopy analysis. Antibodies to CD169 and CD11c were conjugated to CF568 using the Mix-n-Stain CF568 antibody Labeling Kit (Biotium) or using amine-reactive AlexaFluor568-NHS ester (Invitrogen) according to manufacturer instructions.

For multiphoton laser scanning microscopy, we used an Olympus BX51WI fluorescence microscope with a 20 x 1.00 NA water immersion Zeiss objective and dedicated single-beam LaVision TriM Scope II (LaVision Biotec) controlled by Imspector software. The microscope was outfitted with a Chameleon Vision II Ti:Sapphire laser (Coherent) with pulse precompensation. Emission wavelengths were collected with photomultiplier tubes (Hamamatsu) for 412-472 nm (CFP, second harmonic signal), 567-647 nm (RFP), and 500-550 nm (GFP). For 4D analysis of cell migration, stacks of 21 optical sections with 3 µm z-spacing were acquired every 30 sec for 30–60

min with the laser tuned to 900 nm. Each xy plane spanned 512 pixels in each dimension with a resolution of 0.779 µm per pixel. Volocity software (PerkinElmer) was used for 4D tracking of individual cells. All cell tracks were individually examined to confirm that they reported the behavior of a single cell. Volocity and ImageJ were used to create movies of image sequences.

Immunohistochemistry of secondary lymphoid tissue

Popliteal lymph node and spleen were harvested and fixed in periodate-lysine-paraformaldehyde (PLP) Solution (PBS with 100 mM L-lysine, 10 mM sodium M-periodate, 1 % PFA) for 12 h at 4°C. Spleens were reduced to 1-2 mm cross sections before fixation. Tissues were washed in PBS and cryoprotected by an ascending series of 10 %, 20 % and 30 % sucrose in PBS. Samples were snap-frozen in Tissue-Tek OCT Compound (Sakura) and stored at -80°C. Sections of 10 µm, 30 µm, and 50 µm thickness were cut using a Leica Cryostat CM1950 and mounted on Superfrost Plus slides (Fisher). Sections were stained after incubation with Fc receptor blocking peptide (Innovex) and permeabilization with Triton X-100. The following antibodies were used for histological analyses: CD19-eFluor450 (clone 1D3, Ebioscience), B220-eFluor450 (clone RA3-6B2, Ebioscience), CD19-biotin (clone 1D3, BioLegend), B220-biotin (clone RA3-6B2, Biolegend), CD19-A647 (clone 1D3, BioLegend), B220-A647 (clone RA3-6B2, BioLegend), CD3e-A647 (clone 145-2C11, Biolegend), CD169 (clone 3D6.112, Biolegend), CD169-CF568 (clone 3D6.112), and CD11c-A647 (clone N418, BioLegend). Streptavidin-eFluor450 (Ebioscience) and anti-rat-AlexaFluor568 (Invitrogen) were used as secondary detection reagents. Stained sections were embedded in ProLong Gold (Invitrogen) and analyzed by multiphoton laser scanning microscopy (LaVision TriM Scope II) or confocal microscopy (Leica TCS SP5). Optical sections of 1024 pixels in each dimension with a resolution of 0.439 µm per pixel and 1 µm z-spacing were acquired with the LaVision TriM Scope II and images were tiled using Photoshop (Adobe). The wavelength was set to 840 nm (eFluor450, GFP, CF568) or 900 nm (GFP, DsRed). For pLN analysis using Leica TCS SP5, optical sections of 1024x1024 pixels with a resolution of 0.349 µm per pixel and 0.5-1 µm z-spacing were acquired and images were tiled using Leica software. Volocity software (PerkinElmer) was used for image analysis. Distribution of B-1 cells and MLV-infected cells in pLN sections was quantified using Volocity software (PerkinElmer) based on the fluorescence intensity. The number of B-1 cells and MLV-infected cells within the T cell zone, B cell follicles, interfollicular area, T-B cell border, subcapsular sinus floor, and medulla of a pLN was calculated based on CD19/B220 staining of pLN sections (fig. S13D).

Isolation and adoptive transfer of B cells

Naïve mouse B cells were isolated from splenocytes of RFP^+ mice using the EasySep Negative Selection Mouse B Cell Enrichment Kit (StemCell Technologies). Isolated naïve B cells were adoptively transferred by i.v. injection into the tail vein or by s.c. injection into the footpad. B-1 cells were enriched from peritoneal cells of RFP^+ mice by negative selection using biotinylated antibodies against CD4, CD8, CD23, F4/80, Gr-1, TER-119 (BioLegend) and subsequent magnetic separation with Streptavidin RapidSphere magnetic beads (StemCell Technologies). B-1 cells were enriched to over 85 % purity, as confirmed by flow cytometry. Enriched B-1 cells (0.5-1 x 10^6 cells) were adoptively transferred by s.c. injection into the footpad of mice. About 0.3 % of the adoptively transferred B-1 cells reached the draining pLNs accounting for 0.1-0.15 % of total pLN cells. This represents ~25 % of the steady-state B-1 cell population in a pLN.

Fluorescent beads conjugation

1 x 10^8 FluoSpheres NeutrAvidin-conjugated microspheres (0.2 µm, yellow-green fluorescent, Invitrogen) were incubated for 30 min at RT with 1 µg of CD21/CD35 antibody conjugated to biotin (CR2/CR1) (clone 7E9, BioLegend). Antibody-bound fluorescent microspheres were s.c. injected into the footpad of C57BL/6 mice. Draining pLNs were analyzed at different time points post injection by immunhistochemistry.

Clodronate treatment

To deplete SCS macrophages in pLNs, 2.5 µl (12.5 µg clodronate) of clodronate-containing liposomes (CLL) or control liposomes (Encapsula NanoSciences LLC) were s.c. injected into the footpads of C57BL/6 mice. After 14-21 days MLV Gag-GFP capture at the pLN was quantified by flow cytometry 1 h after virus injection. Successful depletion of macrophages in CLL-treated mice was confirmed by flow cytometry analysis (fig. S6A).

SIGN-R1 depletion

To down-regulate SIGN-R1 on cells of pLNs *in vivo* (transient Ab block) (*16*) 12.5 µg of α-SIGN-R1 antibody (clone 22D1, Ebioscience) were s.c. injected into the footpad of C57BL/6 mice 1-2 days before MLV capture experiments. Down-regulation of SIGN-R1 was confirmed by flow cytometry (fig. S8A).

Analysis of CD169 expression

Cells were isolated from collagenase-treated pLNs of C57BL/6 mice using a BD FACSAria sorter. Total RNA was isolated from 20,000-50,000 sorted $CD169^+$ $CD11b^+$ macrophages, $CD5^+$ B-1 cells and $CD5^-$ B cells with the RNEasy Micro Kit (Qiagen) and cDNA was transcribed using the iScript™ cDNA Synthesis Kit (BIORAD). The genes and the primers used for quantitative PCR are as follows: CD169 (forward: 5´-CACCTACAACTTCCGCTTTG-3´; reverse: 5´-TTCCTCTCCATGCCTTCAC-3´), ubiquitin C (forward: 5´-GCCCAGTGTTACCACCAAGA-3´; reverse: 5´-CCCATCACACCCAAGAACA-3´), GAPDH (forward: 5´-TGTGTCCGTCGTGGATCTGA-3´; reverse: 5´-TTGCTGTTGAAGTCGCAGGAG-3´). The PCR reaction was monitored using the iTaq™ universal SYBR® Green supermix (BIORAD) on a Real-Time PCR System (CFX Connect Real-Time PCR Detection System). The relative mRNA abundance of CD169 was determined based on the housekeeping genes ubiquitin C and GAPDH.

To test for an induction of CD169 expression, B-1 cells and macrophages were isolated from the peritoneal cavities of C57BL/6 mice. B-1 cells and macrophages were enriched by negative selection using biotinylated antibodies against CD4, CD8, CD23, F4/80, Gr-1 (B-1 cells) and CD4, CD8, CD19, Gr-1 (macrophages), respectively. Cells were subsequently isolated by magnetic separation with Streptavidin RapidSphere magnetic beads (StemCell Technologies) and stimulated with LPS (2.5 µl/ml), IFNγ (25 ng/ml), IFNα/β (500 U/ml) or co-cultured for 24 h. CD169 expression in cells before and after stimulation was analyzed by flow cytometry.

Determination of neutralizing antibodies in infected mice

MLV_{luc} was generated for neutralization assay by harvesting culture supernatants of HEK293 cells transfected with plasmids encoding full-length MLV Fr57 and MLV LTR-driven firefly luciferase reporter with a packaging signal (MSCV Luciferase PGK-hygro was a gift from Scott Lowe; Addgene plasmid # 18782). Serial two-fold dilutions of indicated heat-inactivated (56°C for 30 min) serum samples of MLV-infected mice were incubated for 1 h at 37 °C with MLV_{luc} (luciferase values corresponding to 2 x 10^4 I.U.) and 1 µl of guinea pig complement (MP Biomedical, 1:64 hemolytic titer) in a total volume of 50 µl in a 96-well plate. S49.1 T cells (2 x 10^5) were then

added to each well and incubated further at 37 °C for 24 h. Sedimented cells were lysed using 1X passive lysis buffer (Promega) and the luciferase activity was measured using a luciferase assay system (Promega) in a Berthold multiwell luminometer. Luciferase activity in samples with pooled sera from uninfected mice was set as 100 %. The data was plotted and analyzed using GraphPad Prism v6.0. The dose-dependent inhibition of MLV infection was fitted on a non-linear regression curve to obtain IC50 values defined as the amount of serum that neutralizes half the MLV infectivity. The IC50 values for each strain of mice for individual time points were analyzed using Two-way Anova with Tukey's multiple comparisons test to determine if they were significantly different from each other.

Sample Preparation for Electron Microscopy

MLV was s.c. injected into footpads of C57BL/6 mice and the draining pLNs were isolated and immediately fixed with 0.1 M sodium cacodylate trihydrate containing 3 % glutaraldehyde, 1 % paraformaldehyde, and 5 % sucrose. Pre-fixed whole lymph nodes were rinsed with fresh cacodylate buffer and placed individually into brass planchettes (Type A; Ted Pella, Inc., Redding, CA) prefilled with 10 % Ficoll in cacodylate buffer. Nodes were covered with the flat side of a Type-B brass planchette and the samples were rapidly frozen with a HPM-010 high-pressure freezing machine (Leica Microsystems, Vienna Austria). The frozen samples were transferred immediately under liquid nitrogen to cryotubes (Nunc) containing a frozen solution of 2.5 % osmium tetroxide, 0.05 % uranyl acetate in acetone. Tubes were loaded into an AFS-2 freeze-substitution machine (Leica Microsystems) and processed at -90°C for 72 h, warmed over 12 h to -20°C, held at that temperature for 6 h, then warmed to 4°C for 2 h. The fixative was removed and the samples rinsed 4 x with cold acetone, following which they were infiltrated with Epon-Araldite resin (Electron Microscopy Sciences, Port Washington PA) over 48 h. Nodes were embedded on Teflon-coated glass microscope slides using Secure-Seal imaging spacers (Sigma-Aldrich) and covered with Thermanox coverslips (Electron Microscopy Sciences). Resin was polymerized at 60°C for 48 h.

Electron Microscopy and Dual-Axis Tomography

Flat-embedded lymph nodes were observed with a stereo dissecting microscope and regions near the edge of the lymph node (for 1-h studies) or from the center portion (for 2-day studies) were extracted with a microsurgical scalpel and glued to the tips of plastic sectioning stubs. Semi-thick (350 nm) serial sections were cut with a UC6 ultramicrotome (Leica Microsystems) using a diamond knife (Diatome, Ltd. Switzerland). Sections were placed on Formvar-coated copper-rhodium slot grids (Electron Microscopy Sciences) and stained with 3 % uranyl acetate and lead citrate. Gold beads (10 nm) were placed on both surfaces of the grid to serve as fiducial markers for subsequent image alignment. Sections were placed in a dual-axis tomography holder (Model 2040, E.A. Fischione Instruments, Export PA) and imaged with a Tecnai TF30ST-FEG transmission electron microscope (300 KeV) equipped with a 2k x 2k CCD camera (XP1000; Gatan, Inc. Pleasanton CA). Tomographic tilt-series and large-area montaged overviews were acquired automatically using the SerialEM software package (*35*). For tomography, samples were tilted +/- 64° and images collected at 1° intervals. The grid was then rotated 90° and a similar series taken about the orthogonal axis. Tomographic data was calculated, analyzed and modeled using the IMOD software package (*36, 37*) on MacPro computers (Apple, Inc., Cupertino, CA). To quantify the frequency of infectious synapses and membrane-rich protrusion contacts, low resolution montaged overviews of pLNs were taken at magnifications suitable for identifying cell types and classifying cellular projections. The identified contacts were then confirmed using high-resolution EM images.

Statistical analysis

Statistical comparisons were performed using GraphPad Prism v6.0 software under the assumption that the samples did not follow a Gaussian distribution for most experiments. For two-group comparisons, either the non-parametric Mann-Whitney test (two-tailed) or the non-parametric Wilcoxon matched-pairs signed rank test was used. For multi-group comparisons, either a two-way ANOVA followed by Tukey's or Sidak´s posttest multiple comparisons adjustment or the non-parametric Kruskal-Wallis test followed by Dunn's posttest multiple comparisons adjustment was used. Exact P values are included in the figures. The applied statistical analyses and the numbers of independent replicates (n) are reported in the figure legends. A difference was interpreted as statistically significant if $P < 0.05$ (two-tailed).

Supplementary Figures:

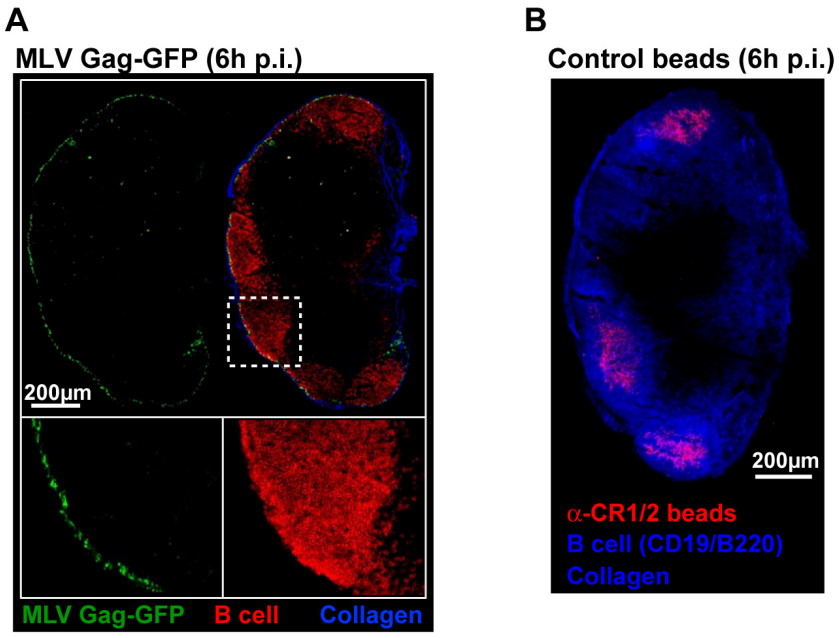

Figure S1 | Virus-sized fluorescent beads displaying antibodies against complement receptor (CR)-1/2 and not MLV Gag-GFP are transported into B cell follicles of pLNs. (**A** and **B**) Immunohistochemistry of pLN sections 6 h after s.c. injection of MLV Gag-GFP (green) (A) or fluorescent beads (~200 nm) conjugated to CR1/2 antibodies (red) (B) into C57BL/6 mice.

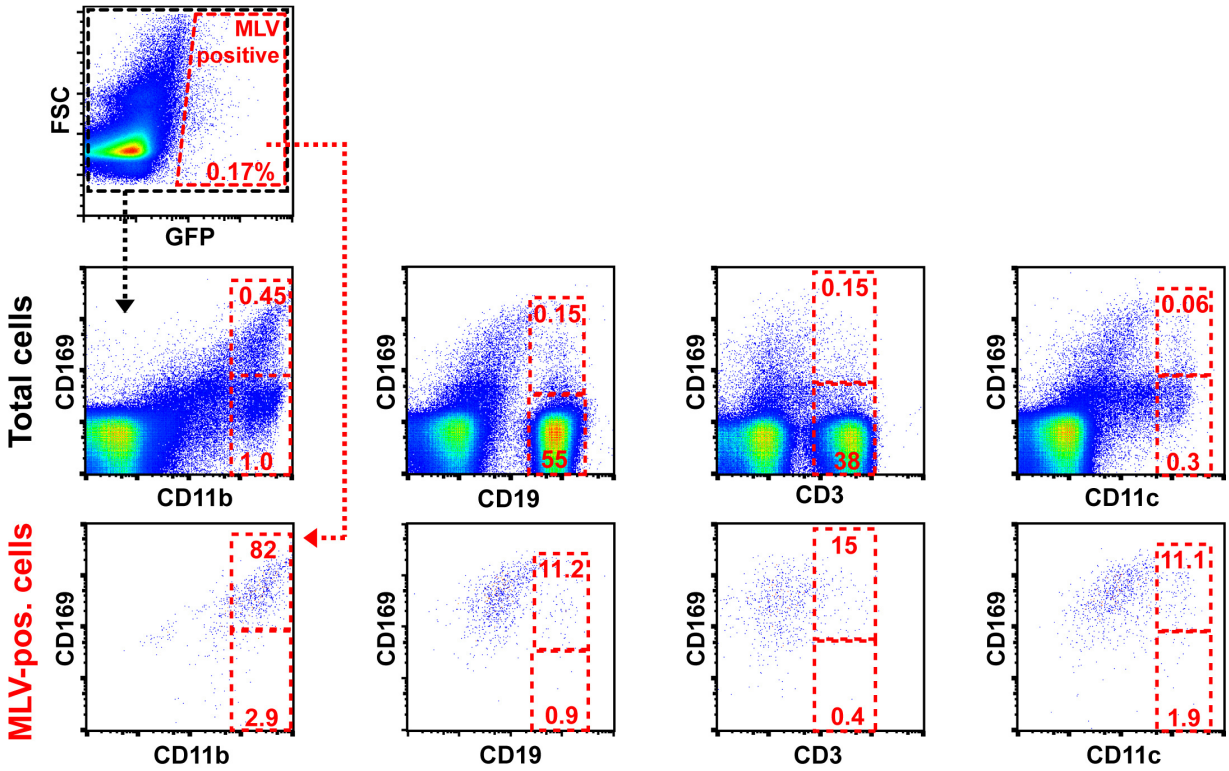

Figure S2 | Flow cytometric analysis of MLV-binding cells at the pLN. Gating strategy for Fig. 1C to identify cells that capture MLV Gag-GFP at the pLN 1 h post s.c. injection. Individual cell types were distinguished by antibody staining for indicated surface markers along with CD169. The total cell-gate was used to select single/double-positive cells within the MLV (GFP)-positive cell population. MLV-positive cells were comprised mainly of $CD169^{+}$ $CD11b^{+}$ macrophages (>80 %).

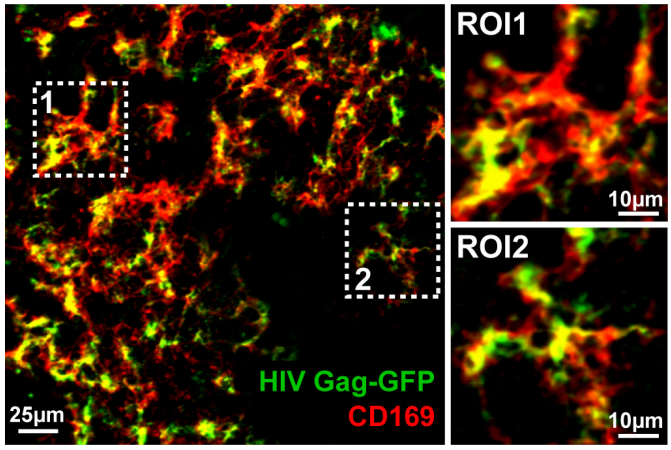

Figure S3 | HIV is captured at the pLN SCS floor by CD169$^+$ macrophages. Intravital 2-Photon laser scanning microscopy (2P-LSM) of HIV Gag-GFP (green) capture by mouse CD169$^+$ macrophages (red) at the pLN SCS floor in C57BL/6 mice. Mouse macrophages were stained by s.c. injection of CF568-conjugated antibodies to CD169 0.5 h post virus injection. ROIs (squares) with HIV (green) and CD169 (red) co-localization are shown to the right.

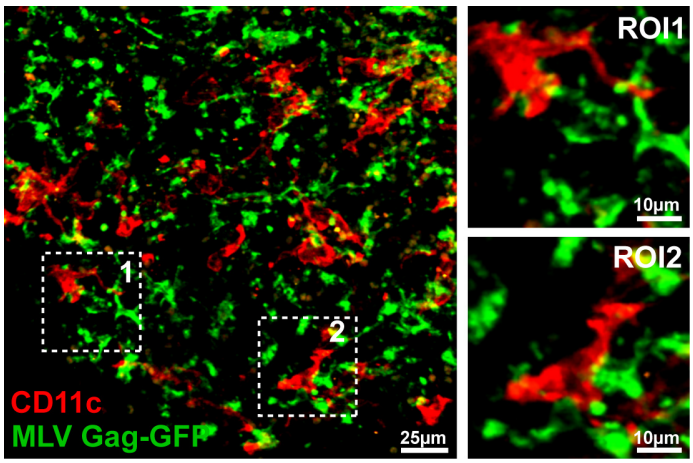

Figure S4 | MLV is not captured at the pLN SCS floor by CD11c$^+$ cells. Intravital 2P-LSM image of MLV Gag-GFP (green) capture and CD11c-expressing cells (red) at the pLN SCS floor. CD11c$^+$ cells were stained by s.c. injection of CF568-conjugated antibodies to CD11c 0.5 h post virus injection. ROIs (squares) with MLV and CD11c distribution are shown to the right.

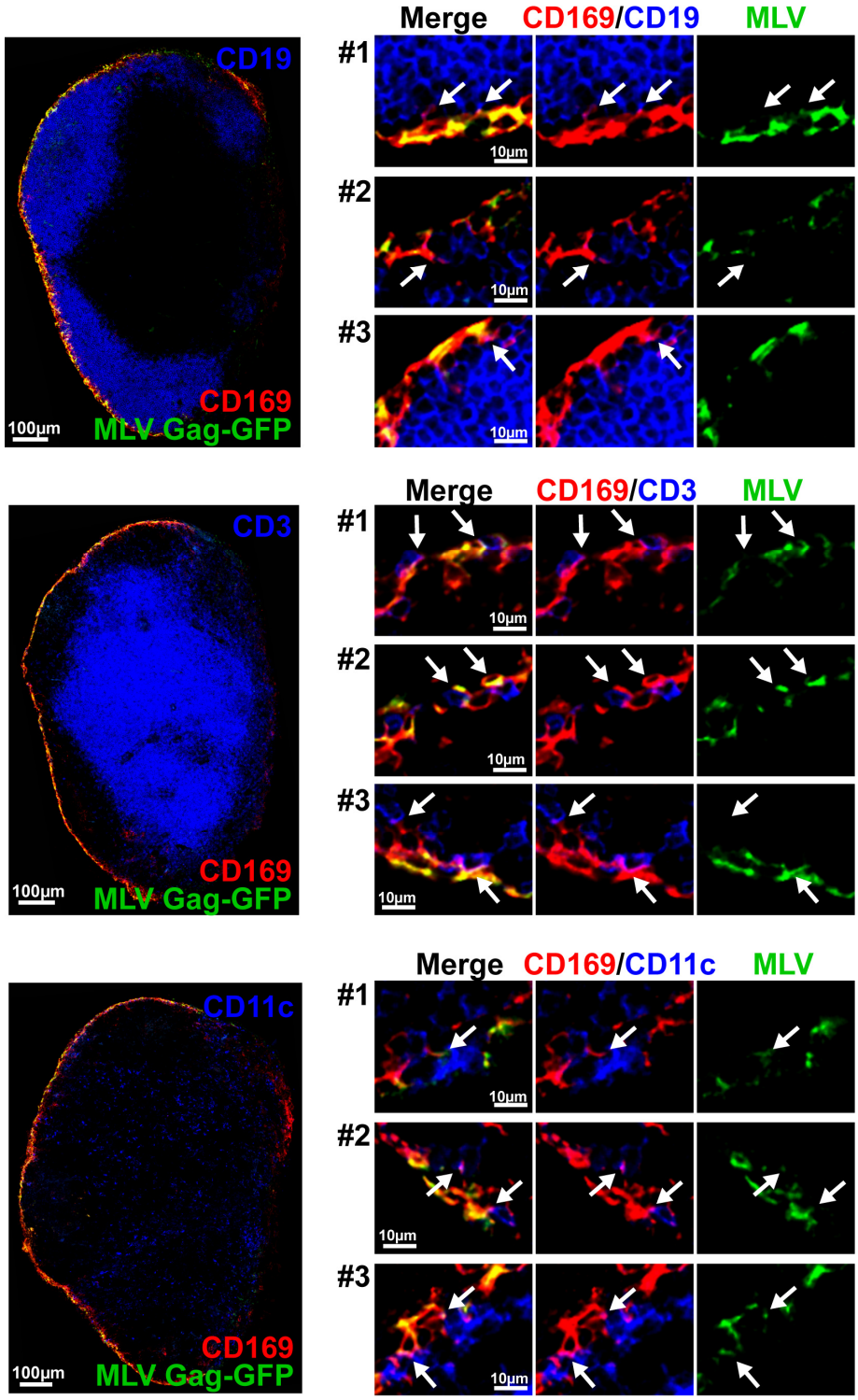

Figure S5 | Immunohistochemical characterization of MLV-binding cells at the pLN SCS floor shows no overlap between CD169 and CD3, CD19 or CD11c. Immunohistochemistry of pLN sections 1 h after s.c. injection of MLV Gag-GFP. Fixed pLN sections (30 µm thickness) were stained with indicated antibodies and the SCS floor analyzed for marker co-localization (ROIs). Arrows highlight contacts between $CD169^+$ macrophages and surface marker-positive cells.

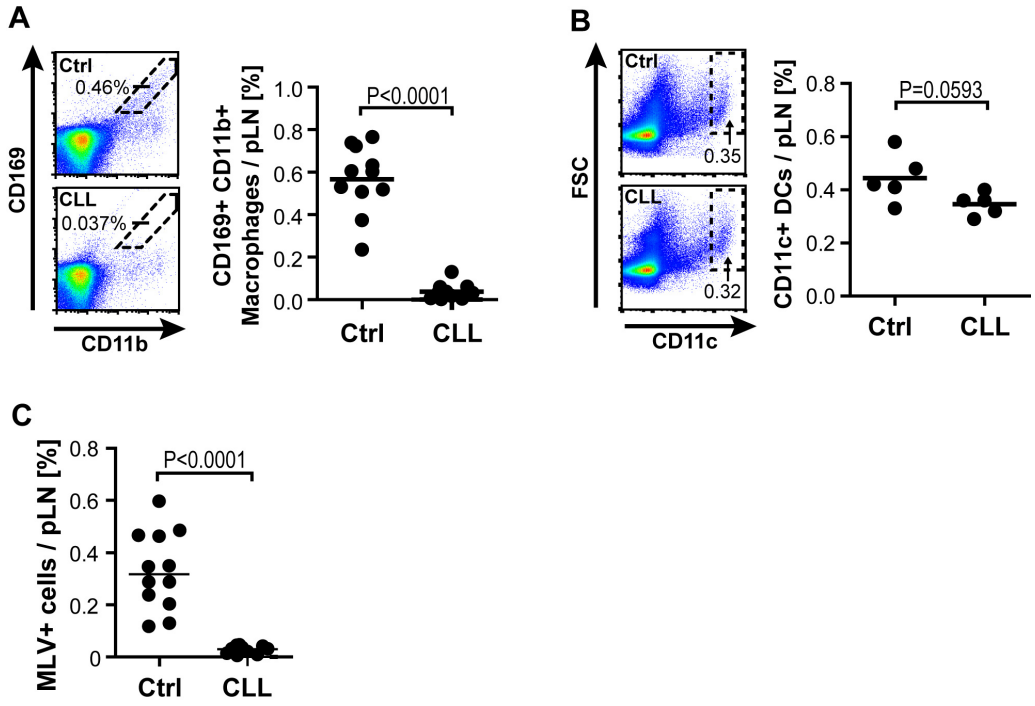

Figure S6 | Macrophage-depletion in pLNs using clodronate-containing liposomes compromises MLV capture. (A and **B)** Representative flow cytometric plots and cumulative data showing the depletion of $CD169^{+}$ $CD11b^{+}$ macrophages (n=12) (A) but not $CD11c^{high}$ DCs (n=5) (B) in pLNs of C57BL/6 mice after s.c. injection of control (ctrl) liposomes or clodronate-containing liposomes (CLL). (**C**) Quantification of MLV Gag-GFP capture at pLNs 1 h after s.c. injection in C57BL/6 mice treated with either control (Ctrl) or clodronate-containing liposomes (CLL) (n=12). Mann-Whitney test, medians are shown.

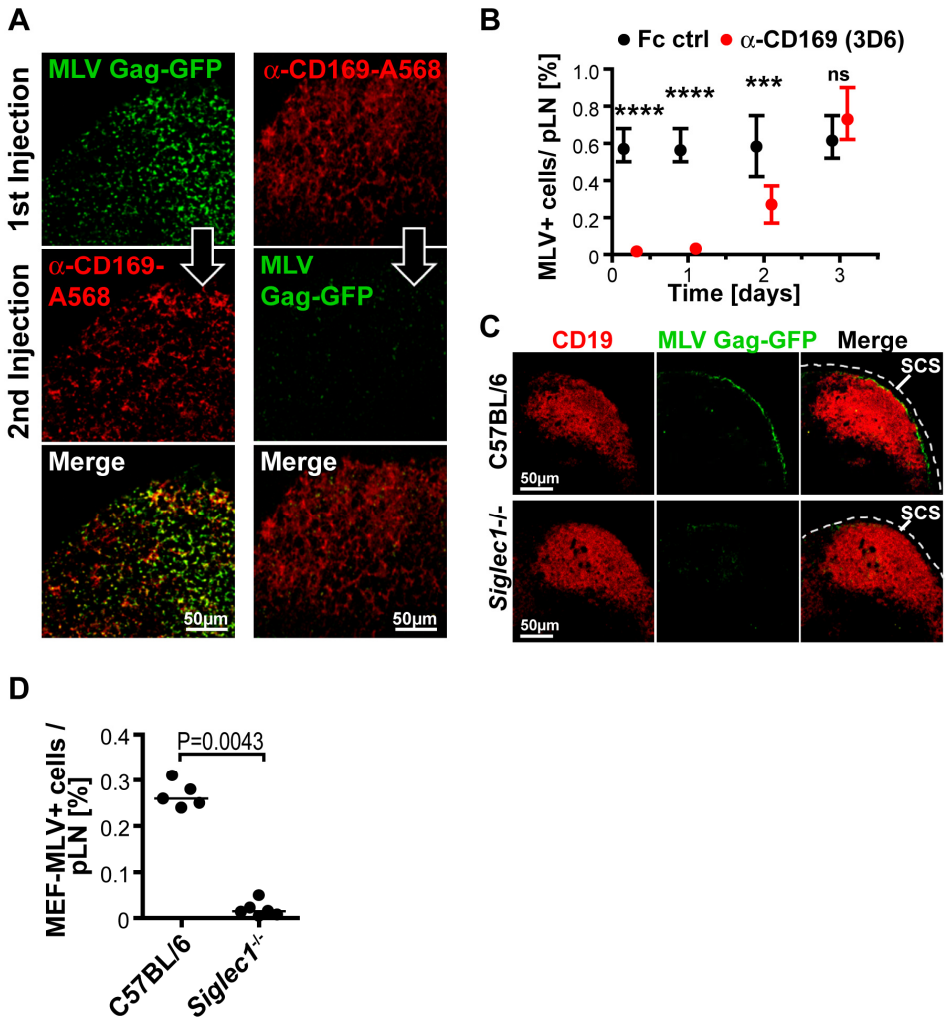

Figure S7 | MLV capture at the pLN SCS floor is dependent on CD169. (**A**) Multiphoton intravital images of MLV Gag-GFP (green) capture by CD169-expressing macrophages (red) at the SCS floor of pLN before or after s.c. injection of antibodies to CD169 conjugated to A568. (**B**) Flow cytometric analysis of MLV Gag-GFP capture at the pLN over time after s.c. injection of CD169 blocking (clone 3D6) or Fc control (Fc ctrl) antibodies. Antibodies were injected 6 h, 1 day, 2 days and 3 days before MLV Gag-GFP. Capture was quantified 1 h after virus injection (n=4 for each time point; Two-way ANOVA followed by Sidak´s multiple comparisons test; ****, P<0.0001; ***, P=0.0006; ns, non-significant; mean ± SEM). (**C**) Immunohistochemistry of a pLN section showing MLV Gag-GFP capture at the SCS floor of C57BL/6 and *Siglec1*$^{-/-}$ mice 1 h after s.c. virus injection. (**D**) Capture of MEF-derived MLV Gag-GFP at the pLNs of C57BL/6 and *Siglec1*$^{-/-}$ mice (n=5-6; Mann-Whitney test).

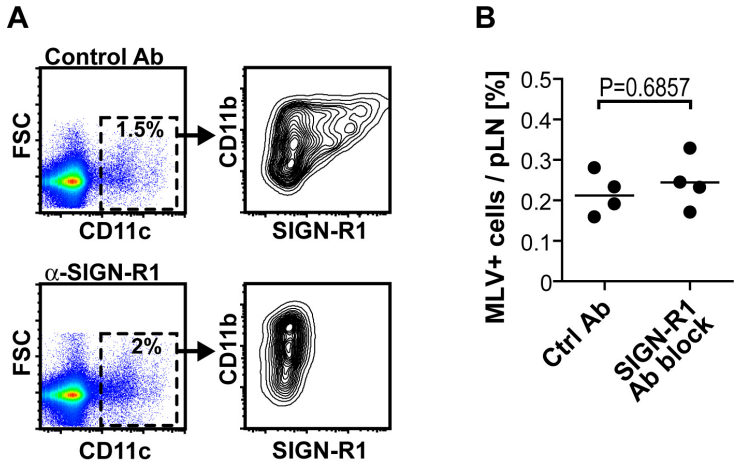

Figure S8 | Transient blockade of SIGN-R1 does not affect MLV capture. (A) Representative flow cytometric plots of SIGN-R1 expressing cells in pLNs of C57BL/6 mice treated with isotype control antibodies or SIGN-R1 antibodies (SIGN-R1). **(B)** Cumulative data showing MLV capture at pLNs after transient blockade (Ab Block) of SIGN-R1 (n=4). Mann-Whitney test, median is shown.

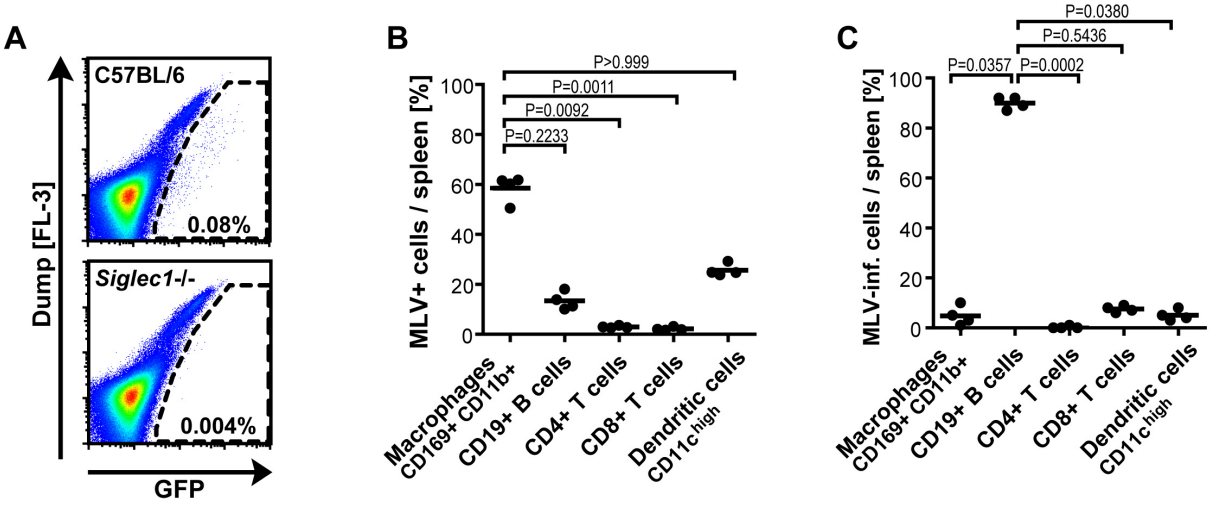

Figure S9 | MLV capture and infection of splenocytes is CD169-dependent. (**A** and **B**) Flow cytometric analysis of MLV Gag-GFP capture at the spleen of C57BL/6 and *Siglec1*$^{-/-}$ mice 0.5 h after i.v. injection. MLV Gag-GFP-binding cells were distinguished based on the indicated surface markers. (**C**) Analysis of MLV LTR-GFP infected splenocytes 2 days after i.v. infection. Kruskal-Wallis with Dunn's multiple comparisons test, medians are shown.

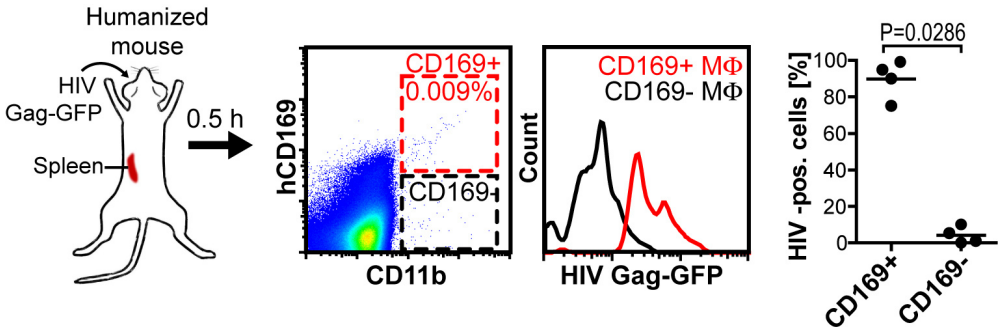

Figure S10 | HIV is captured at the spleen of humanized BLT mice by human CD169$^+$ CD11b$^+$ macrophages. HIV Gag-GFP was i.v. injected into BLT mice and total splenocytes were gated for human CD45$^+$ cells and HIV capture by CD169$^+$ cells was quantified. Mann-Whitney test, median is shown.

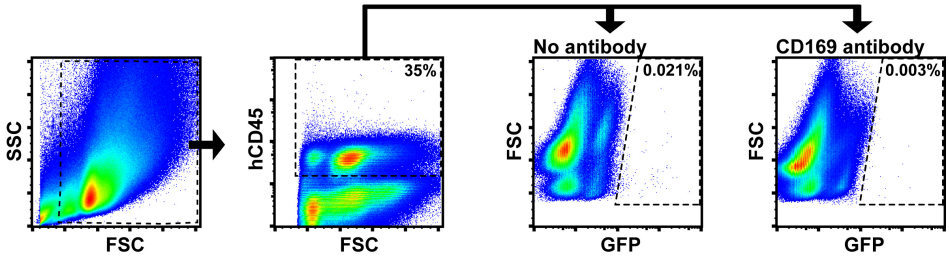

Figure S11 | HIV capture at the spleen of humanized mice. Gating strategy for flow cytometric analysis of HIV Gag-GFP capture at the spleen of BLT mice. Human leukocytes in the spleen were identified based on the surface expression of human CD45 (hCD45) and HIV Gag-GFP particles captured were estimated with or without prior injection of blocking antibodies against CD169.

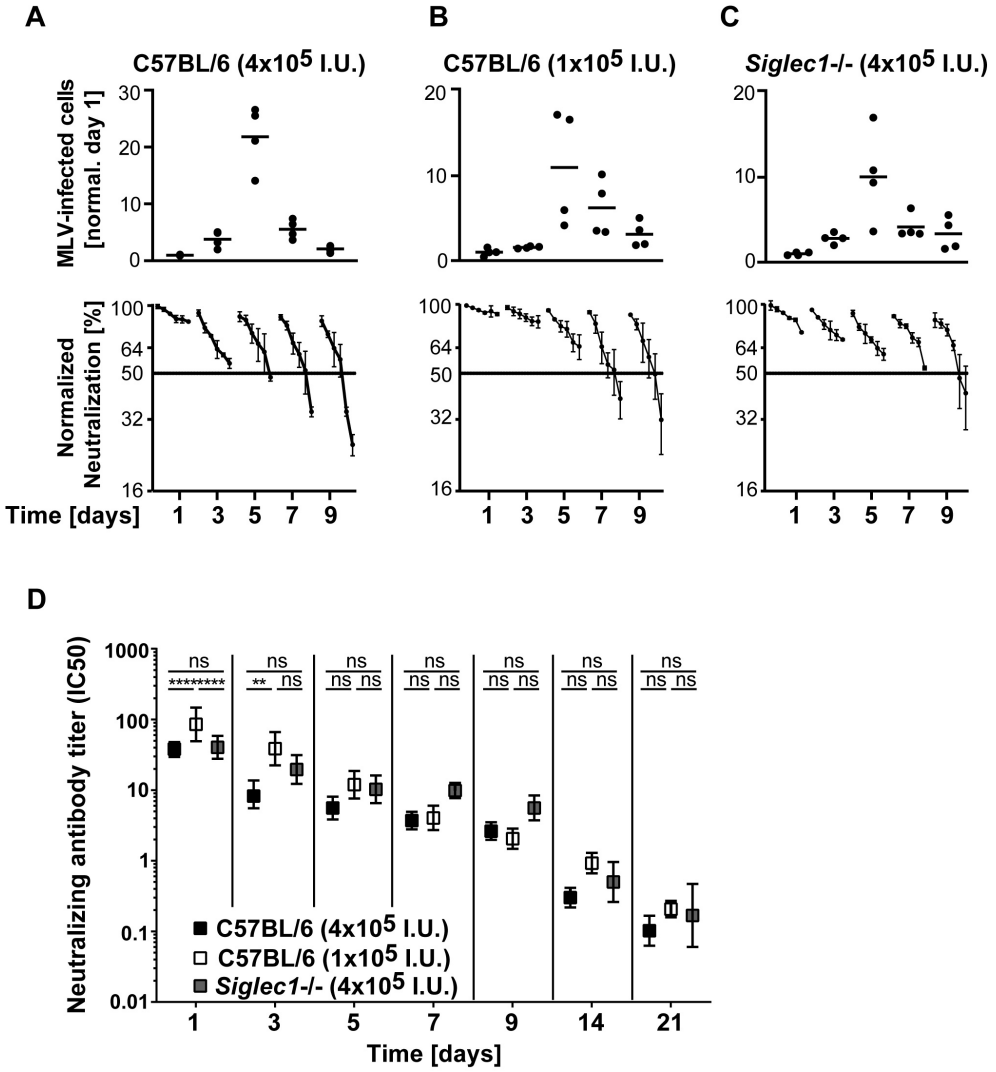

Figure S12 | Production of neutralizing antibodies against MLV is independent of CD169. (**A** to **C**) Upper panels: Total number of MLV-infected cells normalized to that on day 1 in pLNs 1-9 days after s.c. infection with reporter virus MLV LTR-GFP (upper row). C57BL/6 mice were infected with 4 x 10^5 (A) or 1x10^5 (B) infectious units (I.U.) and *Siglec1*$^{-/-}$ mice were infected with 4 x 10^5 I.U. (C) of MLV. Each data point represents a single pLN (n=4). Lower panels: Neutralizing activity in serum from mice infected with MLV LTR-GFP corresponding to the time points in the upper panel. Data depict serial 2-fold dilutions (1/50-1/1600) of sera. The line depicts 50% neutralization and error bars show SD (n=4). (**D**) Analyses of MLV neutralizing antibody titers (IC50) generated in C57BL/6 and *Siglec1*$^{-/-}$ mice after MLV infection (1-21 days). Two-way ANOVA followed by Tukey´s multiple comparisons test; ****, P<0.0001; **, P<0.01; ns, non-significant; mean ± SD are shown.

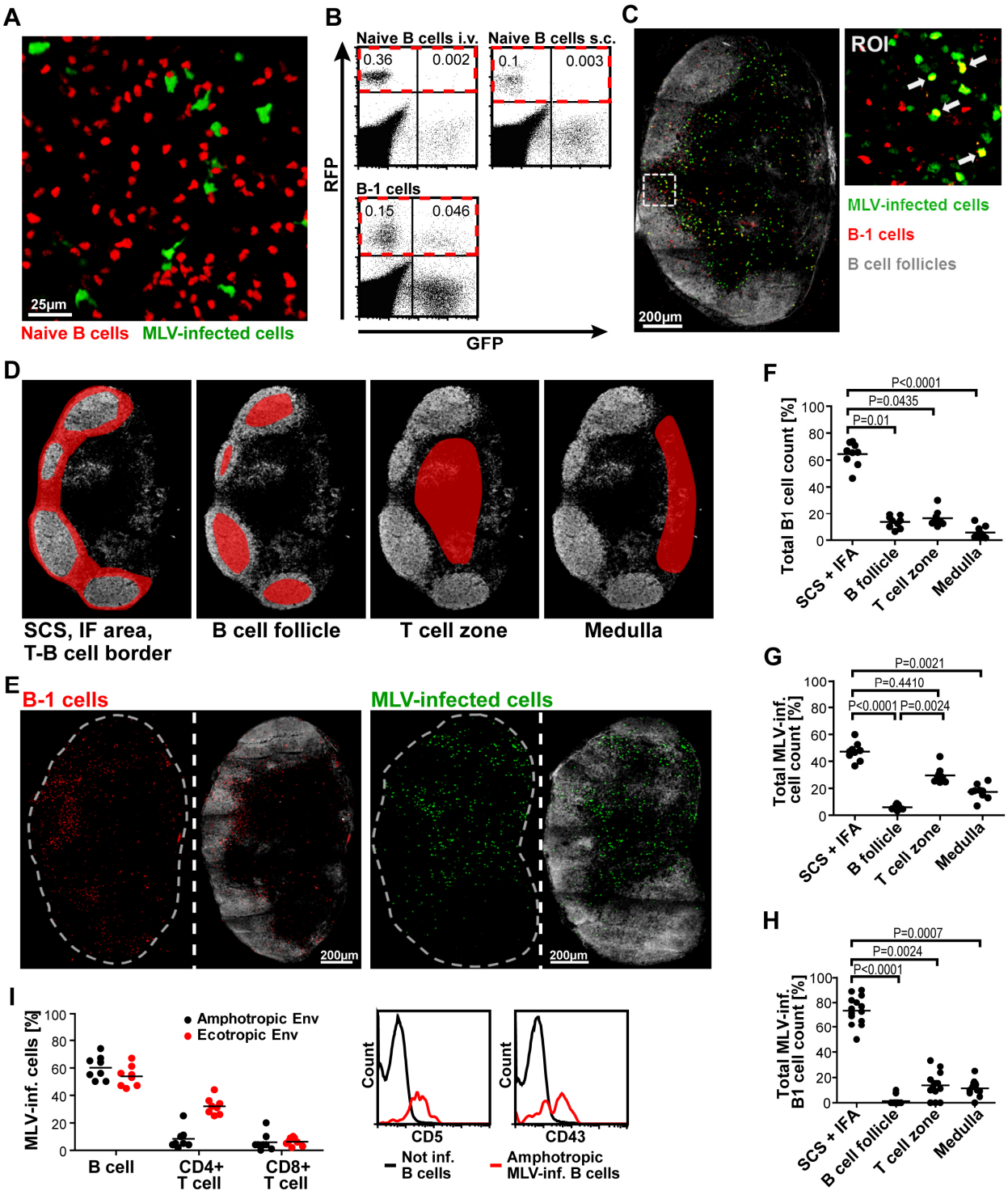

Figure S13 | MLV specifically targets B-1 cells in the pLN SCS floor and the interfollicular area (IFA) to establish infection in mice. (**A**) MLV does not infect naïve B cells. An image from time-lapse intravital movie 4 of a pLN 2 days after s.c. infection with MLV LTR-GFP (green). Naïve B cells (red) isolated from the spleen of RFP$^+$ mice were adoptively transferred (s.c.) 24 h before virus infection. (**B**) Flow cytometric analysis of MLV LTR-GFP-infected pLNs from mice with adoptively transferred naïve RFP$^+$ B cells (i.v. and s.c.) (upper panels) or RFP$^+$ B-1 cells (s.c.) (lower panel). (**C**)

MLV LTR-GFP-infected (green) and RFP$^+$ B-1 cells (red) in a pLN 2 days after infection. B cell follicles in pLN sections were stained with antibodies to CD19/B220 (gray). (**D**) The images depict the strategy used to define areas (shown in red) in histological sections of pLNs based on staining with CD19/B220 antibodies and known distribution of specific cell types. (**E**) Distribution of adoptively transferred RFP$^+$ B-1 cells and MLV LTR-GFP-infected leukocytes in pLNs 2 days after s.c. infection based on the strategy outlined in (D). B cell follicles are shown in gray. (**F** to **H**) Quantification of adoptively transferred B-1 cells (n=9) (F), MLV-infected leukocytes (n=9) (G) and MLV LTR-GFP-infected B-1 cells (n=12) (H) in different areas of pLNs defined as in (D) for an experiment as in (E). Data are from 3 independent experiments with 3-4 pLN sections analyzed for each experiment. Kruskal-Wallis test followed by Dunn's post-test multiple comparisons adjustment. (**I**) Flow cytometry analysis of MLV-infected leukocytes 2 days after s.c. infection with MLV LTR-GFP virus carrying amphotropic or ecotropic Env. Both amphotropic and ecotropic MLV preferentially infect B-1 cells with the ecotropic MLV also infecting some T cells. Cumulative data from pLNs of 8 mice as well as representative flow cytometric plots (right) are shown.

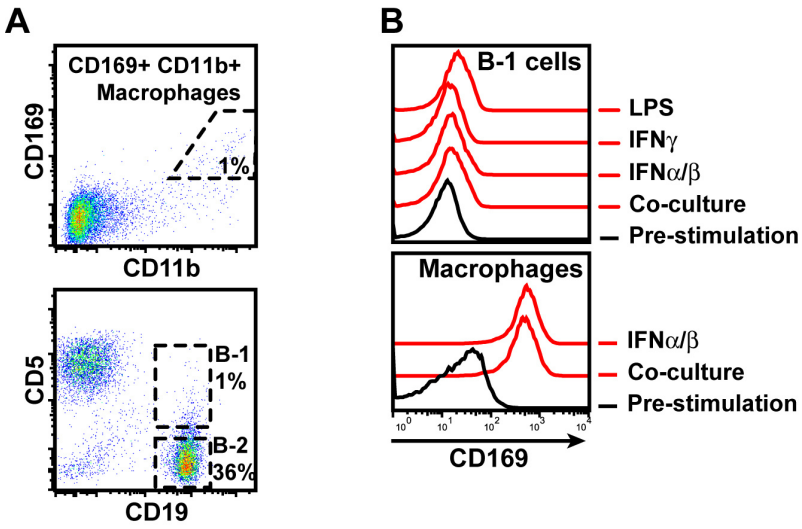

Figure S14 | B-1 cells do not express CD169. (**A**) Gating strategy for the sorting of CD169$^+$ CD11b$^+$ macrophages, CD5$^+$ B-1a cells and CD5$^-$ B cells from pooled pLNs of C57BL/6 mice. Q-PCR analysis for CD169 mRNA in sorted cell populations is shown in Fig. 2C. (**B**) Flow cytometric analysis of CD169 expression in peritoneal B-1 cells and macrophages after *in vitro* activation or mixed culture (co-culture) for 24 h. Cells were fixed and analyzed by flow cytometry.

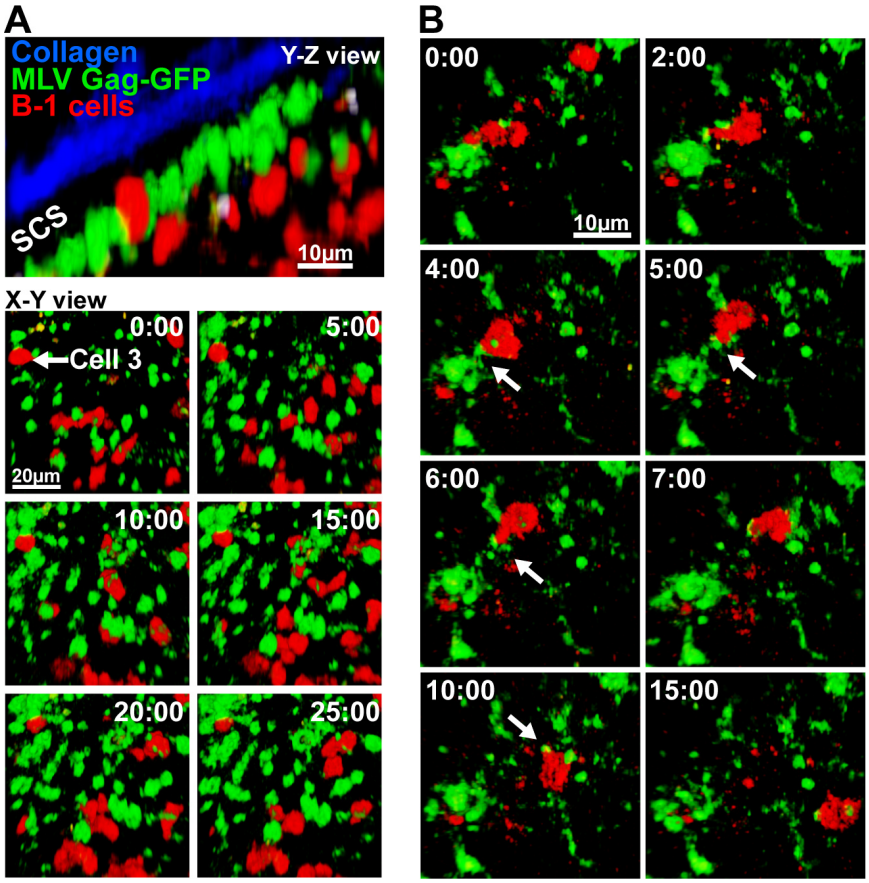

Figure S15 | MLV-laden macrophages at the SCS floor form stable synapses with B-1 cells for virus transfer. (**A**) Image sequence of movie 7 showing stable contacts between RFP^+ B-1 cells (red) and MLV Gag-GFP-laden macrophages (green) at the pLN SCS floor 3 h after s.c. infection. Collagen at the pLN capsule is shown in blue. Analysis of the migration trajectory for cell 3 (arrow) is shown in Fig. 3F. (**B**) Image sequence of movie 9 for MLV Gag-GFP (green) transfer from MLV-laden macrophages to adoptively transferred RFP^+ B-1 cells (red) at the pLN SCS floor. Arrows depict MLV Gag-GFP (green) at the uropod of a migrating RFP^+ B-1 cell (red).

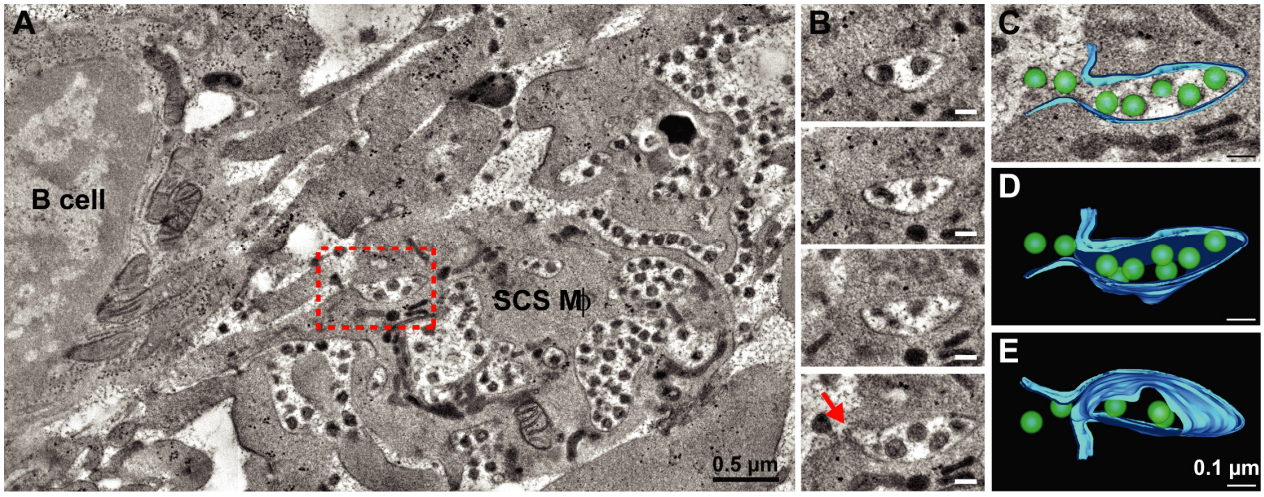

Figure S16 | EM overview of MLV capture at the pLN SCS floor. (**A**) Overview image, taken below the collagen fibrils of a pLN capsule, showing a SCS macrophage in contact with a B cell. (**B** and **C**) Tomographic slices of the SCS macrophage, taken from the region indicated by the red dashed square in (A), showing a MLV-laden cytoplasmic compartment which, in subsequent slices, is shown to be continuous with the invaginated plasma membrane. Arrow in (B) indicates the opening of the invagination to the extracellular space. Scale bar, 0.1 µm. (**D** and **E**) 3D model of the invagination shown in (A, dashed square) and (B); Green spheres, MLV particles; Blue, invaginated plasma membrane.

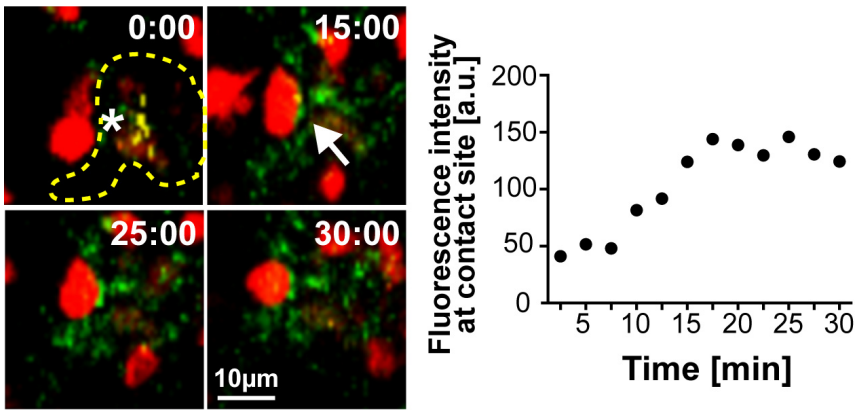

Figure S17 | MLV Gag-GFP accumulates at contact site between a MLV-infected cell and a B-1 cell. Image sequence from movie S12 documenting the accumulation of MLV Gag-GFP at the contact site (asterisk) between a MLV-infected cell (yellow dashed line) and an uninfected RFP^+ B-1 cell (red). Accumulation of fluorescence Gag-GFP at contact site over time is shown on the right. Time in minutes.

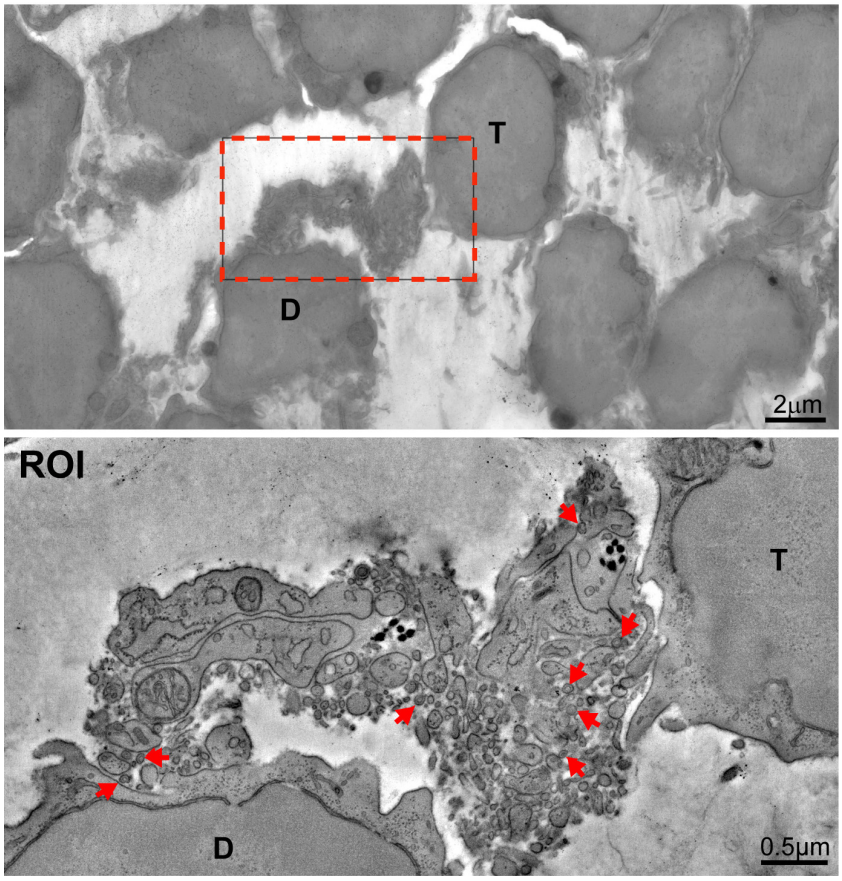

Figure S18 | Uropod-mediated contact between MLV-infected cell and target cell. Electron tomography of MLV-infected pLN tissue 2 days post s.c. infection. The first image is an overview electron micrograph of MLV-containing membranous material in the interface between an infected donor cell (D) and a target cell (T). The second image (ROI) is a tomographic slice prepared from the region indicated in the overview (red square). Arrowheads indicate viral particles along the surface of membranous material emanating from the infected cell.

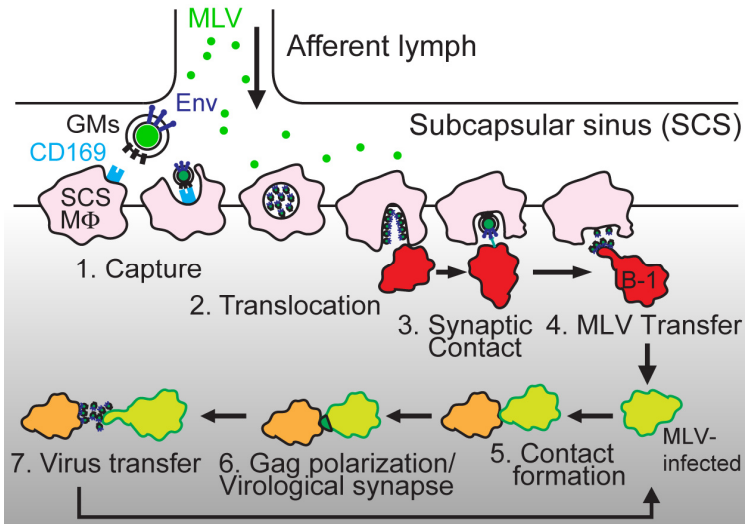

Figure S19 | Model for early events in the establishment of MLV infection in mice. Incoming MLV particles are captured by SCS macrophages through CD169/Siglec-1-dependent recognition of gangliosides (GMs) within the viral lipid bilayer. MLV particles are transferred via synaptic contacts to mCAT-1 expressing B-1 cells. Infected B-1 cells migrate into pLN interior and form Env/receptor-dependent virological synapses to spread the infection.

Captions for Movies S1 to S14

Movie S1 | MLV Gag-GFP is captured at the pLN subcapsular sinus (SCS) floor. 3D rendering of time-lapse intravital 2-Photon laser scanning microscopy (2P-LSM) showing the arrival of MLV Gag-GFP (green) at the SCS floor of a pLN that is outlined by the collagen capsule (blue). The time-lapse was taken every 30 sec in a 3D space of 400 x 400 x 60 µm with 3 µm z-spacing over a period of 60 min after s.c. injection into a C57BL/6 mouse.

Movie S2 | Capture of HIV Gag-GFP at the pLN SCS floor. Time-lapse movie as for movie S1 showing the arrival of HIV Gag-GFP (green) at the SCS floor of a pLN (collagen, blue). The time-lapse video was taken over a period of 40 min following the s.c. MLV injection into a C57BL/6 mouse.

Movie S3 | CD169$^+$ macrophages capture MLV particles at the pLN SCS floor. A z-stack of PFA-fixed pLN 1 h after s.c. injection with MLV Gag-GFP (green). The movie starts at the top of the pLN where the collagen capsule is visible in blue. CD169$^+$ macrophages were stained by injecting CF568-labeled antibodies to CD169 (red) 30 min after virus. Images of pLN explants were taken at a depth of 0-60 µm and a 3D space of 450 x 450 x 60 µm with 1 µm z-spacing.

Movie S4 | MLV does not infect naïve B cells in the pLN. An extended focus projection of time-lapse intravital 2P-LSM of a pLN containing naïve RFP$^+$ B cells (red) 2 days after s.c. infection with MLV reporter virus (MLV LTR-GFP). MLV-infected cells express GFP (green). RFP$^+$ naïve B cells were adoptively transferred 18 h before MLV infection. Note that none of the naïve RFP$^+$ B cells are green and hence are not infected by MLV. Images were taken every 30 sec over a period of 45 min in a 3D space of 300 x 300 x 60 µm with 3 µm z-spacing

Movie S5 | B-1 cells sample the SCS space with MLV-laden macrophages. 3D rendering of time-lapse intravital 2P-LSM at the pLN of a C57BL/6 mouse carrying adoptively transferred RFP$^+$ B-1 cells (red) 2 min after s.c. injection of fluorescently labeled MLV Gag-GFP particles (green). Collagen of pLN capsule is shown in blue. Images were taken every 30 sec in a 3D space of 400 x 400 x 60 µm with 3 µm z-spacing.

Movie S6 | B-1 cells establish synaptic contact with MLV-laden SCS macrophages. 3D rendering of time-lapse intravital 2P-LSM at the pLN of a C57BL/6 mouse as adoptively transferred RFP$^+$ B-1 cells (red) establish synaptic contact with MLV Gag-GFP (green)-laden SCS macrophages 3 h after s.c. injection. Collagen of pLN capsule in blue. Arrows indicate two examples of static B-1 cells in contact with SCS macrophages. Images were taken every 30 sec over a period of 45 min in a 3D space of 200 x 200 x 60 µm with 3 µm z-spacing.

Movie S7 | B-1 cells form stable long-lived synaptic contact with MLV-laden SCS macrophages. 3D rendering of time-lapse intravital 2P-LSM at pLN of mice demonstrating long-lived contact (30 min) of adoptively transferred RFP$^+$ B-1 cells (red) with MLV Gag-GFP (green)-laden SCS macrophages at the pLN SCS 3 h after s.c. injection of virus. Images were taken every 30 sec over 30 min at a 3D space of 110 x 110 x 60 µm with 3 µm z-spacing.

Movie S8 | B-1 cell carrying MLV Gag-GFP material at its uropod following a long-lived interaction with a SCS macrophage. An extended focus projection of time-lapse intravital 2P-LSM in which a RFP$^+$ B-1 cell (red) first interacts with a macrophage and all MLV Gag-GFP (green)

material is concentrated at the cell-cell interface. When the B-1 cell begins to migrate, MLV Gag-GFP (green) material localizes to its trailing uropod. The pLN SCS region was imaged 3 h after s.c. virus injection. Top view (x-y) is shown at the left and sideview (x-z) at the right. Collagen of pLN capsule is shown in blue. Images were taken every 30 sec over a period of 18 min at a 3D space of 90 x 90 x 60 µm (top view) and 12 x 25 x 60 µm (side view) with 3 µm z-spacing.

Movie S9 | Migrating B-1 cells carry MLV particles at its uropod. A time-lapse intravital 2P-LSM for a similar event as in movie S8. The movie lasts over 25 min in a 3D space of 125 x 125 x 60 µm with 3 µm z-spacing.

Movie S10 | Electron tomography of a MLV-laden SCS macrophage. Montaged tomographic reconstruction of a SCS macrophage in a mouse pLN 1 h after s.c. injection of MLV. Large numbers of virus particles are found at the surfaces and in numerous plasma membrane invaginations of the macrophage. Nearly all virus particles are mature. The size bar corresponds to 200 nm.

Movie S11 | MLV-infected B-1 cells form stable virological synapses *in vivo*. An extended focus projection of intravital time-lapse 2P-LSM of pLN 2 days after s.c. infection with replication competent MLV labeled with Gag-GFP. MLV-infected cells express Gag-GFP (green). RFP^+ B-1 cells (red) were adoptively transferred s.c. 18-24 h before MLV infection. Note that incoming MLV Gag-GFP can infect adoptively transferred B-1 cells (red, green) as well as endogenous unlabeled B-1 cells (green). Two regions of interest (ROI1, ROI2) are presented to the right for examples of stable virological synapses with polarized Gag-GFP accumulation in MLV-infected RFP^+ B-1 cells. Images were taken every 30 sec over a period of 30 min in a 3D space of 280 x 280 x 60 µm with 3 µm z-spacing. ROIs are 90 x 90 x 60 µm (ROI1) and 70 x 70 x 60 µm (ROI2) in size.

Movie S12 | Stages of MLV spread *in vivo* via cell-cell contacts. Extended focus projection of intravital 2P-LSM of a pLN 2 days after s.c. infection with replication competent MLV labeled with Gag-GFP. RFP^+ B-1 cells (red) were adoptively transferred through s.c. injection 18-24 h before MLV infection. The left panel shows a MLV-infected cell (green) forming a stable contact with an uninfected B-1 cell (red). The middle panel shows the polarization of Gag-GFP towards the cell-cell interface with a B-1 cell (red). The right panel shows transfer of MLV Gag-GFP material to an unlabeled non-infected endogenous cell. Images were taken every 30 sec over a period of 25-30 min. The 3D space of left, middle and right panel are 80 x 80 x 40 µm, 70 x 70 x 9 µm and 80 x 80 x 45 µm respectively, with 2 µm, 3 µm and 3 µm z-spacingrespectively.

Movie S13 | Electron tomography of a virological synapse. Tomographic reconstruction of virus-containing membrane protrusions in a pLN 2 days post s.c. infection with MLV. This movie corresponds to Figure 3F. The infected donor cell is located to the upper right, outside of the field of view with the uropod extending a considerable distance and curving around other nearby cells. Viruses associated with these protrusions are exclusively immature suggesting that maturation occurs after entry (*38*). The size bar corresponds to 0.5 µm.

Movie S14 | Electron tomography of a MLV containing uropod complex at a virological synapse. Serial-section tomographic reconstruction of a large, virus containing membrane protrusion in a pLN 2 days post s.c. infection with MLV. This movie corresponds to fig. S18. The infected donor cell is at the lower left and the virus containing protrusion extends outward to contact a cell at the upper right. All of the MLV particles within the reconstruction are immature. The size bar corresponds to 0.5 µm.